

Inhibition of the cardiac angiogenic response to exogenous vascular endothelial growth factor

Pierre Voisine, MD, Cesario Bianchi, MD, PhD, Marc Ruel, MD, MPH, Tamer Malik, MD, Audrey Rosinberg, MD, Jun Feng, MD, PhD, Tanveer A. Khan, MD, Shu-Hua Xu, PhD, Jennifer Sandmeyer, BS, Roger J. Laham, MD, and Frank W. Sellke, MD, Boston, Mass

Background. *The angiogenic effects of vascular endothelial growth factor (VEGF) are mediated by the stimulation of endothelial nitric oxide synthase (eNOS) and nitric oxide release. Nitric oxide availability is decreased in patients with coronary disease, a possible explanation for the humble results of VEGF in clinical trials. We sought to examine the effects of exogenous VEGF in a model of endothelial dysfunction.*

Methods. *Miniswine fed either a regular (N = 6, group NORM) or hypercholesterolemic diet (N = 6, HICHOL) underwent ameroid placement on the circumflex artery. Three weeks later, baseline myocardial perfusion was assessed by microsphere injections, and all pigs were treated with VEGF. Four weeks later, microsphere injections were repeated and the hearts harvested. Endothelial-dependent coronary microvascular reactivity, and VEGF and eNOS expression were assessed.*

Results. *HICHOL pigs showed significant endothelial dysfunction in the ischemic territory. Post-treatment myocardial blood flow in the circumflex territory was significantly higher in the NORM compared to the HICHOL group. VEGF and eNOS levels were increased in the ischemic territory in the NORM group but decreased in the HICHOL group.*

Conclusions. *The cardiac angiogenic response to VEGF was markedly inhibited in a hypercholesterolemia-induced porcine model of endothelial dysfunction. Coronary endothelial dysfunction could be an obstacle to the efficacy of clinical angiogenesis protocols and a putative therapeutic target. (Surgery 2004;136:407-15.)*

From the Divisions of Cardiothoracic Surgery and Cardiology, Beth Israel Deaconess Medical Center, Boston, Mass

ANGIOGENIC GROWTH FACTORS have been proposed as an alternative therapeutic strategy for patients with advanced coronary artery disease (CAD) who are not amenable to conventional revascularization techniques. Therapeutic angiogenesis with vascular endothelial growth factor (VEGF) and fibroblast growth factor (FGF)-2 has been used successfully in animal models of ischemia but has shown very modest benefits in clinical trials.^{1,2}

The reasons for the discrepancies between the results from animal and human studies are unclear. However, since VEGF and other angiogenic growth factors operate in large part through the release of endothelial-derived nitric oxide (NO) via the activation of tyrosine kinase receptors,³ the failure of effect seen in patients with CAD, hypercholesterolemia, diabetes, hypertension, and other risk factors for endothelial dysfunction may be related to a deficiency in the stimulated release of NO. The production of NO as well as that of other endothelium-derived substances is significantly altered as a result of the patients' disease state.⁴ In vitro studies suggest an important relationship between the release of NO and the regulation of VEGF-mediated blood vessel growth and development. VEGF enhances the expression of eNOS in native and cultured endothelial cells, an effect which may be important in the process of VEGF-induced angiogenesis;⁵ Endothelial nitric oxide synthase (eNOS) expression is increased in proliferating compared to confluent endothelial

Presented at the 65th Annual Meeting of the Society of University Surgeons, St. Louis, Missouri, February 11-14, 2004.

Supported by grant R01 HL69024 from the National Institutes of Health (F.W.S.). Dr Voisine is a research fellow of the Heart and Stroke Foundation of Canada.

Reprint requests: Frank W. Sellke, MD, Division of Cardiothoracic Surgery, Beth Israel Deaconess Medical Center, 110 Francis St, LMOB 2A, Boston, MA 02215.

0039-6060/\$ - see front matter

© 2004 Elsevier Inc. All rights reserved.

doi:10.1016/j.surg.2004.05.017

cells.⁶ Moreover, inhibitors of NOS suppress angiogenesis, and the proliferative effect of VEGF is decreased in the presence of NOS inhibitors.^{7,8} Meanwhile, in vivo or clinical evidence of the influence of endothelial dysfunction on the angiogenic process within the heart is lacking.

Consequently, we studied in a porcine model the effects of hypercholesterolemia-induced endothelial dysfunction on the angiogenic potential of exogenous VEGF, as well as the molecular mechanisms regulating the angiogenic response in such conditions.

METHODS

Study design. Fifteen Yucatan miniswine (Sinclair Research, Columbia, Mo) were either fed a regular chow ($n = 7$) or a hypercholesterolemic diet ($n = 8$; consisting of 4% cholesterol, 17.2% coconut oil, 2.3% corn oil, 1.5% sodium cholate, and 75% regular chow) starting at 7 weeks of age and continued throughout the entire study period (total period of diet modification of 20 weeks). All animals received humane care in compliance with the Harvard Medical Area Institutional Animal Care and Use Committee and the National Research Council's Guide for the Care and Use of Laboratory Animals, prepared by the Institute of Laboratory Animals and published by the National Institutes of Health (NIH publication No. 86-23, revised 1985). For all surgical procedures, anesthesia was induced with ketamine (10 mg/kg im), thiopental (5-10 mg/kg iv), then thiopental 2.5% to effect. The animals were intubated with a cuffed endotracheal tube, mechanically ventilated at 12 to 20 breaths per minute, and maintained under deep general anesthesia with a gas mixture of oxygen at 1.5-2 L/min and isoflurane at 0.75% to 3.0% concentration. Thirty minutes prior to the end of each survival procedure, a dose of buprenorphine (0.03 mg/kg im) was administered, then a fentanyl patch (4 mg/kg) was placed on the animal and left for the first 48 hours after surgery and subsequently as needed.

At 20 weeks of age, all pigs underwent ameroid constrictor placement. Through a left minithoracotomy in the fourth intercostal space, the pericardium was opened, and a ferromagnetic ameroid constrictor of 1.75 mm in internal diameter was placed around the proximal circumflex coronary artery. Eight million isotope-labeled red-gold microspheres (BioPhysics Assay Laboratory, Worcester, Mass) were injected in the left atrium over a period of 30 seconds during temporary occlusion of the circumflex artery to determine the exact myocardial territory at risk ("shadow-labeling

procedure"). Pleural air was evacuated over a tube thoracostomy, the thoracotomy incision closed, the femoral catheter removed, the femoral artery repaired, and the groin incision closed prior to the animal's emergence from anesthesia.

Three weeks after ameroid insertion, the pigs were again anesthetized as described above. An 8-French introducer was placed in the surgically exposed right femoral artery, and right and left coronary angiograms were recorded to confirm ameroid closure as well as to evaluate baseline collateral development. A left thoracotomy was performed in the fifth intercostal space and the heart was exposed. Microspheres (1.5×10^7) were injected over 30 seconds in the left atrium with concomitant withdrawal of 16 mL of blood in 2 minutes from the femoral arterial catheter, both at rest (samarium) and under pacing at 150 bpm (lanthanum) for perfusion analysis. In all pigs, VEGF administration was then started via an osmotic pump system (ALZET, model 2MLA; Alza, Palo Alto, Calif) delivering a total of 2 μ g of human recombinant VEGF₁₆₅ (R&D Systems, Minneapolis, Minn) mixed with 50 U of heparin in 2 mL of saline at a rate of 3 μ L/h through a microcatheter secured within the myocardium adjacent to the circumflex artery.

Four weeks after initiation of treatment, a coronary arteriography was performed via left femoral access under general anesthesia. The heart was exposed through a sternotomy; microspheres (lutetium at rest and ytterbium under pacing) were then injected and blood withdrawn as described above. Euthanasia was performed with 10 mL/kg of a saturated KCl solution administered intravenously. The heart was harvested and two 1-cm-thick transversal slices were cut at the midventricle level, then sectioned into 8 segments identified clockwise starting from the anterior junction of the right and left ventricles. Samples from the anterior and left lateral walls were snap frozen in liquid nitrogen for molecular studies, put in 4°C Krebs solution for in vitro assessment of microvessel reactivity, weighed and dried for microsphere perfusion analyses, or fixed in 10% formalin for histology.

In vitro assessment of coronary microvessel reactivity. After cardiac harvest, epicardial coronary arterioles (70-150 μ m in diameter and 1-2 mm in length) originating from branches of the left anterior descending and circumflex arteries were dissected from the surrounding tissue with a $\times 40$ dissecting microscope and examined in isolated organ chambers as described previously.⁹ The responses to sodium nitroprusside (SNP) (1 nmol/L-100 μ mol/L), an endothelium-independent

cGMP-mediated vasodilator, as well as to adenosine 5' diphosphate (ADP) (1 nmol/L-10 μ mol/L) and VEGF (1 fmol/L-1 nmol/L), 2 endothelium-dependent receptor-mediated vasodilators that act via bioavailable NO, were studied.¹⁰

Perfusion analysis. Myocardial blood flows were determined during each procedure with isotope-labeled microspheres (ILMs) (BioPAL, Worcester, Mass) by previously reported methods.¹¹ ILMs of different isotopic mass were used at each experimental stage: Red (gold-labeled) microspheres were injected during temporary circumflex occlusion at the time of ameroid placement to identify myocardial samples that originated from the circumflex coronary distribution (those with the lowest count of gold-labeled microspheres). Black (samarium-labeled) and blue (lanthanum-labeled) ILMs were used during the second procedure respectively at rest and under pacing at 150 bpm to determine baseline blood flow in the lateral territory 3 weeks after ameroid placement, at the time of VEGF treatment administration. Pink (lutetium-labeled) and green (ytterbium-labeled) ILMs were injected at rest and during pacing at the final procedure, 4 weeks after instauration of VEGF therapy. Following euthanasia, 10 circumferential, transmural left ventricular sections were collected for ILM assays in each animal, weighed, and dried. Each sample was exposed to neutron beams and microsphere densities measured in a gamma counter. Adjusted myocardial blood flows, reflecting changes in lateral myocardial perfusion during VEGF treatment, were determined from the myocardial samples that showed respectively the highest (left anterior descending [LAD] distribution) and the lowest (circumflex distribution) count of red microspheres. We then calculated the ratios of blood flow in the collateral-dependent territory compared to the control anterior wall and compared the post- versus pretreatment phase using the following equation: blood flow post-treatment/blood flow pretreatment = pink/black (at rest), or = green/blue (under pacing).

Immunohistochemistry. Myocardial samples from the circumflex territory of pigs from both groups were stained with CD31 antibody (BD Biosciences Pharmingen, San Diego, Calif), counterstained with methyl green, and examined for capillary endothelial cell density in a triplicate, blinded fashion from $700 \times 550 \mu\text{m}$ (0.385 mm^2), randomly selected, left ventricular cross-sectional fields, according to methods reported previously.¹¹

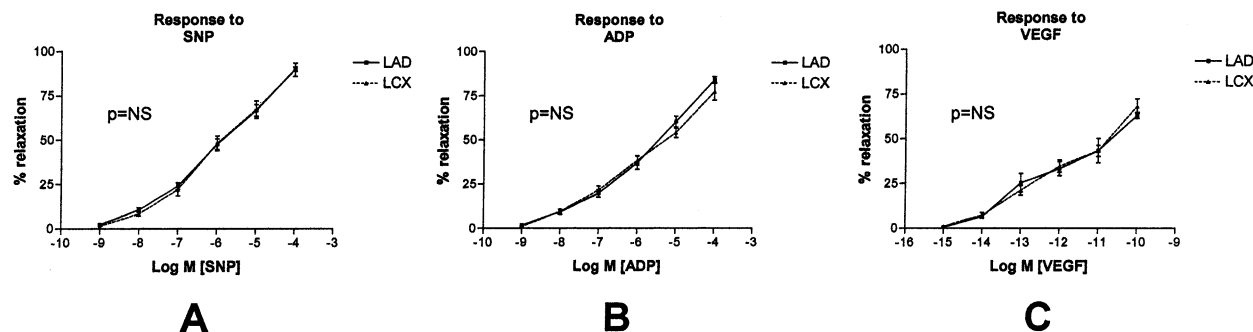
Western blot analysis. Whole-cell lysates were isolated from the homogenized anterior and lateral myocardial amples with a RIPA solution (Biotech,

Ashland, Mass) and centrifuged at 12,000g for 10 minutes at 4°C to separate soluble from insoluble proteins. The supernatant protein concentration was measured spectrophotometrically at a 595-nm wavelength with a DC protein assay kit (Bio-Rad, Hercules, Calif). Forty micrograms of total protein were fractionated by 4% to 20% gradient, SDS-polyacrylamide gel electrophoresis (Invitrogen, San Diego, Calif) and transferred to PVDF membranes (Milipore, Bedford, Mass). VEGF was detected by incubating the membrane with a 1:1000 dilution of polyclonal antihuman VEGF antibody (Oncogene, Boston, Mass) for 2 hours, followed by incubation with horseradish peroxidase-conjugated, goat antimouse immunoglobulin G (1:3000) for 1 hour. eNOS was detected with 1:1000 dilution of anti-eNOS antibody (Cell Signaling, Beverly, Mass). Immune complexes were visualized with the ECL detection system (Amersham, Piscataway, NJ). Bands were measured by densitometric quantification of autoradiograph films.

Northern blot analysis. Myocardial samples from the anterior and lateral myocardial territories were homogenized for 60 seconds on ice; total RNA was then isolated with a Tri-Reagent solution (Sigma, St. Louis, Mo). A 10- μ g RNA pellet was dissolved in RNase free water, fractionated on a 1.3% formaldehyde-agarose gel, and transferred to a GeneScreen Plus filter (Perkin Elmer, Boston, Mass). Complementary DNA probes of VEGF receptor-1 and VEGF receptor-2 were labeled with $\alpha^{32}\text{P}$ -dCTP (Amersham, Arlington Heights, Ill) with the use of a random-priming labeling kit (Boehringer, Indianapolis, Ind) and purified from unincorporated nucleotides with G-50 Quick Spin Columns (Boehringer). The specific activity of the probes used was 1 to 2×10^9 cpm/ μ g. The blots were hybridized at 68°C for 16 hours in UltraHyb solutions (Ambion, Austin, Tex). After hybridization, the blots were washed twice in $2 \times \text{SSC}$, placed in 0.1% SDS for 15 minutes at room temperature, and then re washed twice in $0.1 \times \text{SSC}$, 0.1% SDS for 15 minutes at 60°C. Autoradiography was carried out at -80°C for 16 to 20 hours.

Data analysis. Data are reported as mean \pm SEM. Microvessel responses are expressed as percent relaxation of the precontracted diameter and were analyzed by fitting a linear regression model examining the relationship between vessel relaxation, log concentration of the vasoactive agent of interest, and the experimental group or myocardial territory of origin (SAS Version 8, Cary, NC). Immunoblottings and Northern blots were analyzed after digitalization of x-ray films with the use of a flat-bed scanner (ScanJet 4c; Hewlett Packard,

Normal diet group



High cholesterol diet group

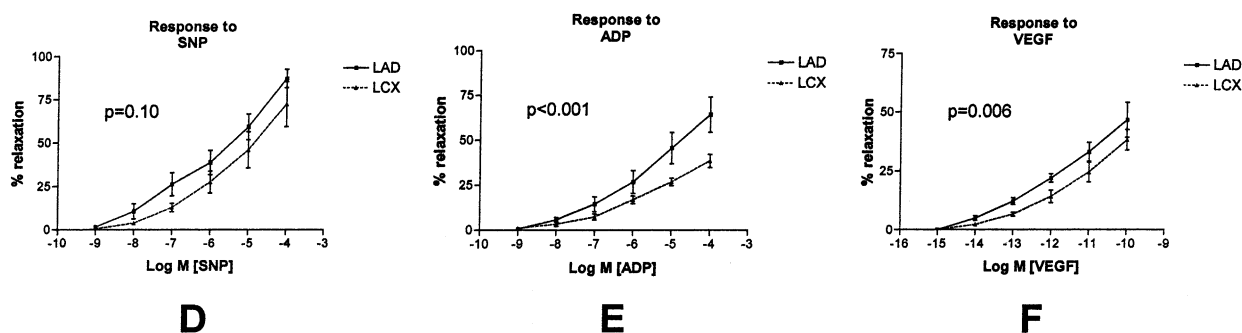


Fig 1. Microvascular reactivity studies. Percent relaxation to increasing concentrations of vasodilating agents after precontraction with U46619. **A-C**, Normal diet group: responses to endothelium-independent vasodilator SNP (**A**) and to endothelium-dependent vasodilators adenosine diphosphate (ADP) and VEGF (**B**, **C**). **D-F**, High-cholesterol diet group: responses to SNP (**D**), ADP (**E**), and VEGF (**F**). *P* values show significance of the difference between left circumflex (LCX) and LAD responses to the different agonists.

Palo Alto, Calif) and NIH Image 1.62 software (National Institute of Health, Bethesda, Md). Comparisons between samples were analyzed by 1-way ANOVA followed by a 2-tail *t* test using Microsoft Excel (Microsoft Corporation, Seattle, Wash). Values are expressed as mean fold change \pm SEM. Ponceau S staining and ethidium bromide were used to determine proper fractionation and equivalent loading of proteins and RNA, respectively. Only samples with similar fractionation and loading less than 20% differences were analyzed further. The optical density ratio of the bands to that of Ponceau S and ethidium bromide were used to correct for small uneven loading (<20%).

RESULTS

Animal model. One pig from the normal diet group died 2 days after ameroid placement, probably from arrhythmia. Two pigs from the HICHOL group died (1 at 24 hours after ameroid

placement, the other at the time of the treatment procedure [VEGF treatment]) from acute heart failure after pacing at 150 bpm, eventually leading to ventricular fibrillation that was unresponsive to pharmacologic intervention and defibrillation. Serum cholesterol levels were significantly higher in the HICHOL group at the time of ameroid placement (390 ± 12 vs 89 ± 9 mg/dL, $P < .01$), at the onset of VEGF administration (507 ± 39 vs 86 ± 11 mg/dL, $P < .01$) and at the time of harvest (778 ± 65 vs 90 ± 15 mg/dL, $P < .01$). Coronary angiograms confirmed the complete closure of the ameroid constrictors in all animals, with impaired distal filling of the circumflex (TIMI 2 flow). There was no significant difference in the visible collateral vessel development between the 2 groups.

Microvessel reactivity. Figure 1 shows the relaxation curves to increasing concentrations of vasodilators after precontraction with the thromboxane/prostaglandin endoperoxide analogue U46619. Endothelial dysfunction in the high-cholesterol

diet group was evidenced by the significantly impaired vasorelaxation to ADP and VEGF, 2 endothelium-dependent vasodilators, in the circumflex distribution ($P < .001$ and $P = .006$ vs the LAD territory, respectively; Fig. 1, E, F). Relaxation to the endothelium-independent agent SNP showed a trend to a decreased response in the ischemic area, although it did not reach statistical significance ($P = .10$, Fig. 1, D). In contrast, there was no difference in the curve responses from the circumflex and LAD territories in the normal diet group (Fig 1, A, B, C).

Myocardial perfusion. The results of isotope-labeled microsphere assays in determining circumflex myocardial perfusion are depicted in Fig 2. Three weeks after ameroid placement, at the time of VEGF treatment initiation, baseline circumflex coronary flow was similar between the 2 diet groups, both at rest (0.61 ± 0.07 vs 0.54 ± 0.05 mL/min/g, Normal vs High cholesterol groups, $P = .42$) and under pacing (0.59 ± 0.07 vs 0.55 ± 0.04 mL/min/g, Normal vs High cholesterol groups, $P = .58$). After 4 weeks of VEGF therapy, at the time of the final procedure, circumflex myocardial blood flow both at rest and under pacing was significantly higher in the normal diet group than in the high-cholesterol counterpart. Respective ratios of blood flow in the circumflex to the LAD territories in the post- versus pretreatment settings were 1.18 ± 0.05 (normal diet) versus 1.00 ± 0.06 (high-cholesterol diet) at rest ($P = .04$), and 1.16 ± 0.10 (normal diet) versus 0.80 ± 0.05 (high-cholesterol diet) under pacing ($P = .009$), thus corresponding in increases from baseline perfusion of 18% and 16% for the normal diet group respectively at rest and under pacing, while the high-cholesterol group showed no improvement at rest and a decrease of 20% under pacing.

Capillary endothelial density. Figure 3 shows the density of CD 31-positive capillary endothelial cells in the left lateral wall of pigs from both diet groups 4 weeks after initiating VEGF treatment. The cell density was significantly higher in the normal diet compared to the high-cholesterol diet groups (87.9 ± 12.2 vs 48.3 ± 10.5 , $P < .01$).

Western blot analysis. Myocardial VEGF and eNOS protein expression were significantly different between the 2 diet groups. Densitometry ratios of VEGF protein levels in the ischemic to the non-ischemic territories were respectively 1.25 ± 0.13 and 0.84 ± 0.16 for the normal and high-cholesterol diet groups ($P < .05$), while the ratios of eNOS protein levels were respectively 1.49 ± 0.25 and 0.86 ± 0.12 ($P = .04$). Both VEGF and eNOS protein levels were thus increased in the ischemic territory

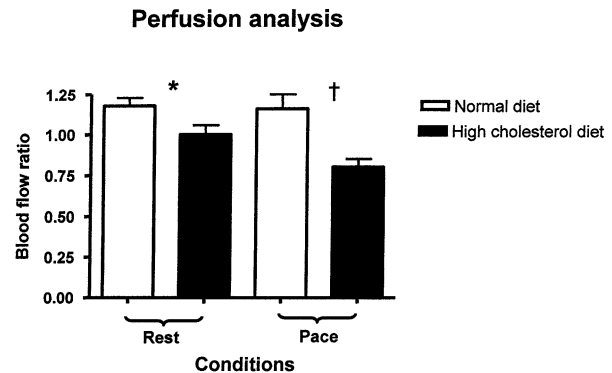


Fig 2. Perfusion analyses. Post- versus pre-VEGF treatment ratios of LCX versus LAD blood flows in normocholesterolemic and hypercholesterolemic pigs. The ratio was significantly higher in the normal diet group both at rest (1.18 ± 0.05 vs 1.00 ± 0.06 , Normal vs High cholesterol groups, $*P = .04$) and under stress by pacing at 150 bpm (1.16 ± 0.10 vs 0.80 ± 0.05 , Normal vs High cholesterol groups, $\dagger P = .009$).

from the normal diet group, but both were decreased in the high-cholesterol diet group. Representative images are displayed in Figure 4.

Northern blot analysis. Expression of VEGF receptor-1 and receptor-2 messenger RNA were also significantly different between the diet groups. Densitometry ratios of the circumflex to LAD territory for VEGF receptor-1 were 0.87 ± 0.07 in the normal diet group compared to 1.03 ± 0.05 in the high-cholesterol group ($P < .05$), while the respective ratios for VEGF receptor-2 were 1.25 ± 0.06 and 0.88 ± 0.05 ($P = .03$) (Fig 5).

DISCUSSION

In this study, significant coronary microvessel endothelial dysfunction was induced in a swine model of chronic ischemia by administration of a cholesterol-rich diet. This dysfunction was associated with a markedly decreased functional response to the angiogenic effects of exogenous VEGF and an altered expression of key molecules in the VEGF-signaling pathway, as compared to pigs undergoing the same VEGF treatment but kept on a regular diet.

The induction of endothelial dysfunction by diet modification with cholesterol enrichment has been described in previous studies. Pigs fed a hypercholesterolemic diet for as little as 9 weeks have been shown to display attenuated endothelium-dependent relaxation to serotonin despite the absence of intimal proliferative changes;¹² 10 weeks of this

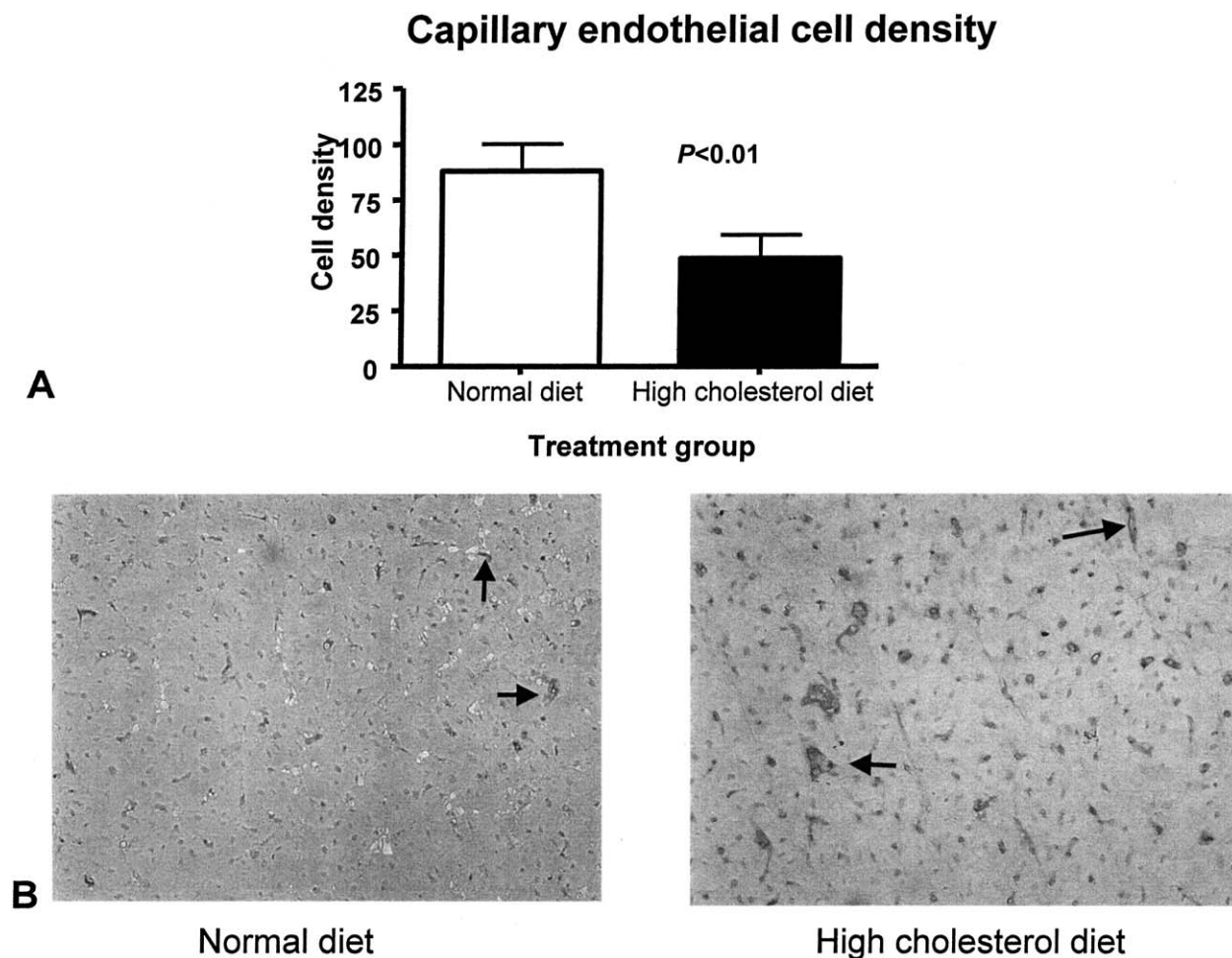


Fig 3. Capillary endothelial cell density. **A**, LCX territory endothelial cell density after VEGF treatment in normocholesterolemic versus hypercholesterolemic pigs. The density was significantly higher in the normal diet group (87.9 ± 12.2 vs 48.3 ± 10.5 , $P < .01$). **B**, Immunohistochemistry for CD31 after VEGF treatment in the LCX territory of a normocholesterolemic (*left*) versus hypercholesterolemic (*right*) pig. Arrows point to microvessels.

diet has also been associated with reduced vasorelaxation to bradykinin.¹³ Although pigs from our study clearly showed impaired vasorelaxation to ADP and VEGF, both endothelium-dependent vasodilators, there also was a tendency toward a decreased response to SNP, an endothelium-independent agent. This finding suggests a partial contribution from the smooth muscle cell-mediated vasodilatation to the observed response in our model. The observed effect could also be explained in part by an accelerated degradation of SNP-derived NO by the increased superoxide anion production associated with hypercholesterolemia.

Increased oxidative stress resulting from the induction of xanthine oxidase, NADH/NADPH oxidase, and uncoupling of eNOS with inactivation from reactive oxygen species have been proposed

to explain the relationship between hypercholesterolemia and endothelial dysfunction.¹⁴ In our study, we observed an inverse response in eNOS and VEGF expression in the circumflex-dependent territory of pigs from the high-cholesterol diet group; this group showed decreased eNOS and VEGF expression, while the normal diet group showed an increase in both. This finding is in accordance with a substantial association between VEGF and eNOS in orchestrating the multiplication, growth, and stabilization of vascular cells in vessel development. The downregulation in eNOS expression could explain the results of a previous report showing that patients with stable CAD and those having suffered acute myocardial ischemia—two clinical situations associated with endothelial dysfunction—experience a diminished release of NO in response to VEGF.¹⁵ Consideration of the

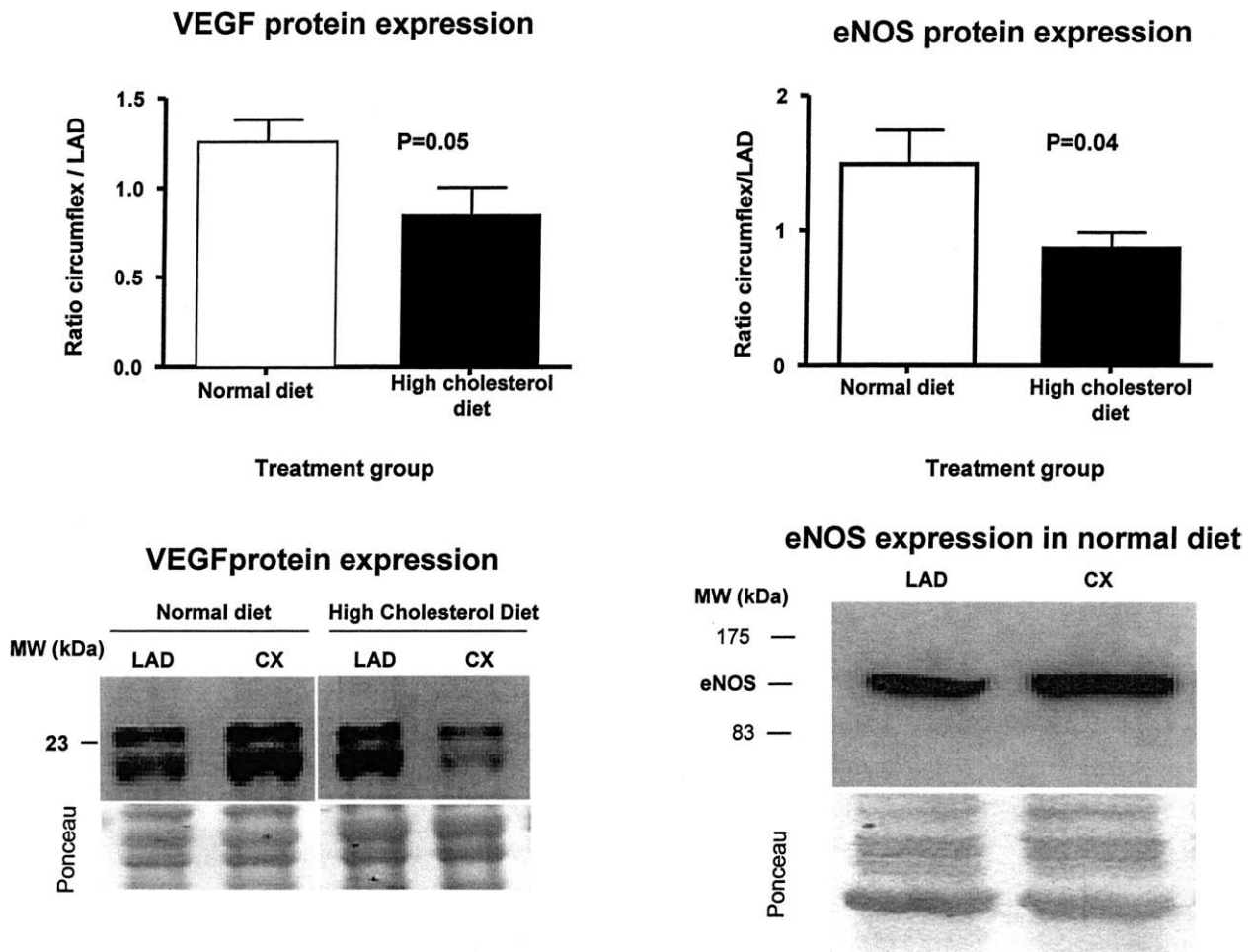


Fig 4. Western blot analysis of VEGF (*left panel*) and eNOS (*right panel*) protein levels in normocholesterolemic and hypercholesterolemic pigs after VEGF treatment. Representative images and bar graphs summarizing expression in the ischemic circumflex territory are shown. Ponceau S optical density was used as a correction factor for quantification. Lateral myocardial VEGF and eNOS protein levels were significantly lower in the high-cholesterol diet group. Ratios of left lateral /left anterior wall VEGF protein expression were 1.25 ± 0.13 and 0.84 ± 0.16 for the normal and high-cholesterol diet groups ($P < .05$), while the ratios for eNOS protein levels were respectively 1.49 ± 0.25 and 0.86 ± 0.12 ($P = .04$).

significantly impaired angiogenic response to exogenous VEGF evidenced in our model of hypercholesterolemia-induced endothelial dysfunction by decreased perfusion and capillary endothelial cell density, and also the critical importance of NO release in the VEGF-mediated angiogenic response suggests a central role for eNOS in the molecular events involved in the altered angiogenic process associated with endothelial dysfunction.

Furthermore, a recent study by Bussolati et al¹⁶ has reported that VEGF-stimulated NO release is inhibited by the blockade of VEGF receptor 1 (VEGFR-1) and that VEGFR-1, via NO-dependent mechanisms, negatively regulates VEGFR-2-mediated endothelial cell proliferation and promotes

formation of capillary networks in human umbilical vein endothelial cells. Consequently, these authors have suggested that VEGFR-1 may be a signaling receptor that promotes endothelial cell differentiation into vascular tubes, in part by limiting VEGFR-2-mediated endothelial cell proliferation via NO, which seems to be a molecular switch for endothelial cell differentiation. The expected increase in VEGFR-1 expression seen in the ischemic area of hypercholesterolemic pigs from our study suggests that the limiting step in the signaling cascade of VEGF not only may be dependent on the downregulation of VEGF expression itself, but also may lie downstream from VEGF receptor activation, again incriminating eNOS as a determining regulator of the angiogenic process. We have not

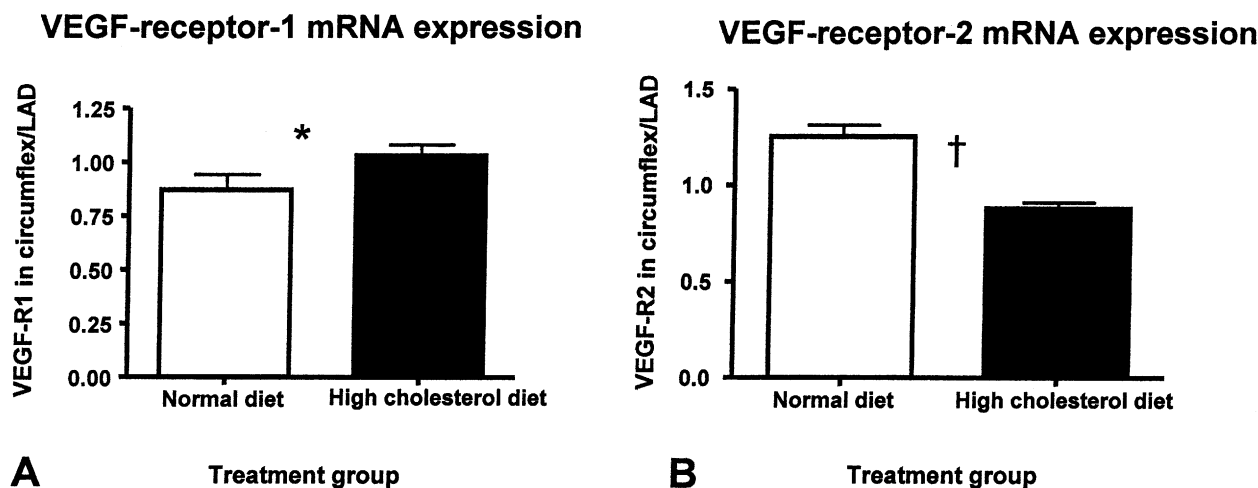


Fig 5. Northern blot analysis of VEGFR-1 (**A**) and VEGFR-2 (**B**) messenger RNA expression in normocholesterolemic and hypercholesterolemic pigs after VEGF treatment. Bar graphs summarizing expression in the ischemic circumflex territory compared to the control anterior (LAD) wall are shown. Ribosomal 18S subunit was used as a correction factor for quantification. Densitometry ratios of the circumflex to LAD territory for VEGFR-1 were 0.87 ± 0.07 in the normal diet group compared to 1.03 ± 0.05 in the high-cholesterol group ($*P = .05$), while the respective ratios for VEGFR-2 were 1.25 ± 0.06 and 0.88 ± 0.05 ($\dagger P < .03$).

measured other metabolites that could be, in part, responsible for hypercholesterolemia-induced inhibition of VEGF-mediated angiogenesis, such as free fatty acids, asymmetric dimethylarginine, oxidized lipids or caveolin; the absence of information on their relative contribution is a limitation to our study.

In a similar experimental design comparing 2 groups of pigs under the same diet regimen, we have previously shown that hypercholesterolemia-induced endothelial dysfunction significantly impairs fibroblast growth factor (FGF)-2-mediated myocardial angiogenesis.¹⁷ It is believed that FGF-2-induced angiogenesis is dependent on Syndecan-4/PKC α and relatively independent of Src kinases, in contrast to VEGF-induced angiogenesis, which invariably involves serine phosphorylation/activation of eNOS and the generation of NO in endothelial cells.¹⁸ Although this may result in a considerably different mechanistic link between the action of each of these growth factors and the local availability of NO, which is likely secondary to key differences in their respective signal transduction pathways, endothelial dysfunction is the common denominator of growth factor-mediated angiogenesis inhibition in both of these studies.

Taken together, these results suggest a paramount role for endothelial integrity in the success of protein growth factor-based therapeutic angiogenesis, a condition that is lacking in patients with

advanced CAD who have thus far been the target of this form of treatment. This finding may explain the discrepancy observed to date between animal and clinical studies testing therapeutic angiogenesis, and warrants the use of more appropriate research models displaying some degree of endothelial dysfunction. Since NO release is mainly regulated by the availability of its substrate, L-arginine, and the activity of eNOS, it also suggests a putative role for combination therapy in which growth factors would be used in conjunction with synthetic NO donors, eNOS activators, antioxidants, or L-arginine itself. To this end, recent studies in apoE- hypercholesterolemic mice exhibiting attenuated collateral vessel formation in response to a FGF-2 disk angiogenesis system and hindlimb ischemia, respectively,^{19,20} which was fully reversed by the oral administration of L-arginine in both instances, provide further support for the evaluation of endothelial function-directed treatment in combination with therapeutic angiogenesis for end-stage CAD patients.

REFERENCES

1. Simons M, Bonow RO, Chronos NA, Cohen DJ, Giordano FJ, Hammond HK, et al. Clinical trials in coronary angiogenesis: issues, problems, consensus: An expert panel summary. *Circulation* 2000;102:E73-86.
2. Henry TD, Annex BH, McKendall GR, Azrin MA, Lopez JJ, Giordano FJ, et al. The VIVA trial: Vascular endothelial

- growth factor in Ischemia for Vascular Angiogenesis. *Circulation* 2003;107:1359-65.
3. Sellke FW, Wang SY, Stamler A, Lopez JJ, Li J, Simons M. Enhanced microvascular relaxations to VEGF and bFGF in chronically ischemic porcine myocardium. *Am J Physiol* 1996;271:H713-20.
 4. Werns SW, Walton JA, Hsia HH, Nabel EG, Sanz ML, Pitt B. Evidence of endothelial dysfunction in angiographically normal coronary arteries of patients with coronary artery disease. *Circulation* 1989;79:287-91.
 5. Bouloumie A, Schini-Kerth VB, Busse R. Vascular endothelial growth factor up-regulates nitric oxide synthase expression in endothelial cells. *Cardiovasc Res* 1999;41:773-80.
 6. Arnal JF, Yamin J, Dockery S, Harrison DG. Regulation of endothelial nitric oxide synthase mRNA, protein, and activity during cell growth. *Am J Physiol* 1994;267:C1381-8.
 7. Ziche M, Morbidelli L, Masini E, Amerini S, Granger HJ, Maggi CA, et al. Nitric oxide mediates angiogenesis in vivo and endothelial cell growth and migration in vitro promoted by substance P. *J Clin Invest* 1994;94:2036-44.
 8. Ziche M, Morbidelli L, Choudhuri R, Zhang HT, Donnini S, Granger HJ, et al. Nitric oxide synthase lies downstream from vascular endothelial growth factor-induced but not basic fibroblast growth factor-induced angiogenesis. *J Clin Invest* 1997;99:2625-34.
 9. Tofukuji M, Metais C, Li J, Franklin A, Simons M, Sellke FW. Myocardial VEGF expression after cardiopulmonary bypass and cardioplegia. *Circulation* 1998;98:II242-6; discussion II247-8.
 10. Sellke FW, Tofukuji M, Laham RJ, Li J, Hariawala MD, Bunting S, et al. Comparison of VEGF delivery techniques on collateral-dependent microvascular reactivity. *Microvasc Res* 1998;55:175-8.
 11. Ruel M, Sellke FW, Bianchi C, Khan TA, Faro R, Zhang JP, et al. Endogenous myocardial angiogenesis and revascularization using a gastric submucosal patch. *Ann Thorac Surg* 2003;75:1443-9.
 12. Cohen RA, Zitnay KM, Haudenschild CC, Cunningham LD. Loss of selective endothelial cell vasoactive functions caused by hypercholesterolemia in pig coronary arteries. *Circ Res* 1988;63:903-10.
 13. Hasdai D, Mathew V, Schwartz RS, Holmes DR, Jr., Lerman A. The effect of basic fibroblast growth factor on coronary vascular tone in experimental hypercholesterolemia in vivo and in vitro. *Coron Artery Dis* 1997;8:299-304.
 14. Cai H, Harrison DG. Endothelial dysfunction in cardiovascular diseases: the role of oxidant stress. *Circ Res* 2000;87:840-4.
 15. Metais C, Li J, Simons M, Sellke FW. Effects of coronary artery disease on expression and microvascular response to VEGF. *Am J Physiol* 1998;275:H1411-8.
 16. Bussolati B, Dunk C, Grohman M, Kontos CD, Mason J, Ahmed A. Vascular Endothelial Growth Factor Receptor-1 Modulates Vascular Endothelial Growth Factor-Mediated Angiogenesis via Nitric Oxide. *Am J Pathol* 2001;159:993-1008.
 17. Ruel M, Wu GF, Khan TA, Voisine P, Bianchi C, Li J, et al. Inhibition of the cardiac angiogenic response to surgical FGF-2 therapy in a swine endothelial dysfunction model. *Circulation* 2003;108(suppl 1):II335-40.
 18. Cross MJ, Claesson-Welsh L. FGF and VEGF function in angiogenesis. Signaling pathways, biological responses and therapeutic inhibition. *Trends Pharmacol Sci* 2001;22:201-7.
 19. Duan J, Murohara T, Ikeda H, Katoh A, Shintani S, Sasaki K, et al. Hypercholesterolemia inhibits angiogenesis in response to hindlimb ischemia: nitric oxide-dependent mechanism. *Circulation* 2000;102:III370-6.
 20. Jang JJ, Ho HK, Kwan HH, Fajardo LF, Cooke JP. Angiogenesis is impaired by hypercholesterolemia: role of asymmetric dimethylarginine. *Circulation* 2000;102:1414-9.